Irradiation induces bone injury by damaging bone marrow microenvironment for stem cells

Xu Cao[a,1], Xiangwei Wu[a,b], Deborah Frassica[c], Bing Yu[a], Lijuan Pang[a,b], Lingling Xian[a], Mei Wan[a], Weiqi Lei[a], Michael Armour[d], Erik Tryggestad[d], John Wong[d], Chun Yi Wen[e], William Weijia Lu[e], and Frank J. Frassica[a,1]

Departments of [a]Orthopaedic Surgery, [c]Radiation Oncology and Molecular Radiation Sciences, and [d]Radiation Oncology Medical Physics, Johns Hopkins University School of Medicine, Baltimore, MD 21205; [b]Shihezi Medical College, Shihezi University, Shihezi Xinjiang 832002, China; and [e]Department of Orthopaedics, University of Hong Kong, Hong Kong 999777, China

Edited* by Peter N. Devreotes, Johns Hopkins University School of Medicine, Baltimore, MD, and approved December 16, 2010 (received for review October 14, 2010)

Radiation therapy can result in bone injury with the development of fractures and often can lead to delayed and nonunion of bone. There is no prevention or treatment for irradiation-induced bone injury. We irradiated the distal half of the mouse left femur to study the mechanism of irradiation-induced bone injury and found that no mesenchymal stem cells (MSCs) were detected in irradiated distal femora or nonirradiated proximal femora. The MSCs in the circulation doubled at 1 week and increased fourfold after 4 wk of irradiation. The number of MSCs in the proximal femur quickly recovered, but no recovery was observed in the distal femur. The levels of free radicals were increased threefold at 1 wk and remained at this high level for 4 wk in distal femora, whereas the levels were increased at 1 wk and returned to the basal level at 4 wk in nonirradiated proximal femur. Free radicals diffuse ipsilaterally to the proximal femur through bone medullary canal. The blood vessels in the distal femora were destroyed in angiographic images, but not in the proximal femora. The osteoclasts and osteoblasts were decreased in the distal femora after irradiation, but no changes were observed in the proximal femora. The total bone volumes were not affected in proximal and distal femora. Our data indicate that irradiation produces free radicals that adversely affect the survival of MSCs in both distal and proximal femora. Irradiation injury to the vasculatures and the microenvironment affect the niches for stem cells during the recovery period.

CFU-fibroblast | repopulation | differentiation | self-renewal | angiography

Ionizing radiation is often used to treat malignancies such as breast cancer, lymphoma, Ewing sarcoma, soft tissue sarcomas, and rectal and anorectal carcinomas. Bone insufficiency is a significant problem resulting in stress fractures, bone fragmentation, and joint dissolution (1, 2). The risk of a hip fracture for a women following pelvic irradiation for the treatment of carcinomas of the anus, cervix, or rectum is as much as three times that of the population of women who do not receive irradiation (3). Women older than the age of 65 y have a 16% lifetime risk of a hip fracture. Fractures of the sacrum are also very common following irradiation. These stress or insufficiency fractures are difficult to treat, with very high rates of delayed union and nonunion of the fractures. Only small amounts of bone healing (i.e., callus) is noted on serial radiographs. Surgical treatment with internal fixation and conventional bone grafting has had only limited success. The mechanism of irradiation-induced bone injury has not been fully elucidated.

Human bone marrow contains both hematopoietic stem cells (HSCs) and the stromal cell compartments; the latter comprises various cell types, including mesenchymal stem cells (MSCs) (4, 5). The MSCs derived from adult bone marrow are pluripotent and can differentiate into heart, lung, and gut epithelia in the animal (6–8). Repopulation with bone marrow-derived MSCs could lead to differentiation into different cell types, including osteoblasts, adipocytes, chondrocytes, and fibroblasts (5). The microenvironment in the bone marrow comprises vascular niche and stromal cell niche including osteoblasts for stem cell self-renewal and differentiation (9, 10). Bone marrow is extremely vulnerable to cytotoxicity caused by radiation therapy (11). In contrast to HSCs, very few data have been published on the radiosensitivity of MSCs. Several recent studies have reported that MSCs from patients exhibit a complete host profile after total body irradiation and bone marrow transplantation, whereas cells differentiated from HSCs are of donor origin (12, 13). However, the cellular and molecular mechanisms accounting for such radiation tolerance in MSCs remain elusive.

Radiation generates free radicals and reactive oxygen species, which damage vital cellular targets such as DNA and membranes, and affect the niches for stem cells (14). Both HSCs and MSCs are implicated in the repair of irradiation damage of distal epithelial through their mobilization in the circulation (15–17). In this study, we aimed to investigate how irradiation affects bone marrow stem cells and residing microenvironment directly or indirectly by using a unique Small Animal Radiation Research Platform (SARRP) built by the Department of Radiation Oncology at Johns Hopkins University, in which computed tomography (CT), X-ray, and irradiation are integrated into a single system (18). We found that irradiation damaged the bone marrow microenvironment for stem cells, and our findings suggest that prevention of the damage during radiation therapy will be helpful for the recovery of bone injury.

Results

To investigate the mechanism of irradiation-induced bone injury, we irradiated mouse femora by using a unique SARRP (Fig. 1*A*). The irradiation can be delivered at an accuracy of 1 mm resolution with the aid of micro-CT and X-ray. Groups of mice were irradiated at the distal half of the femora with a dose of 4 Gy once per day for 5 d consecutively. The left half of the proximal femora and the right femora did not receive irradiation as controls (Fig. 1 *B* and *C*). Histologic staining of the femoral sections showed that irradiation induced adipogenesis in the irradiated left distal femur at 1 wk relative to the right nonirradiated femur. Adipocytes were significantly increased at 4 wk after radiation in the medullary cavity (Fig. 1*D*). The results indicate that irradiation changes the bone marrow microenvironment.

We then examined whether irradiation injured bone and bone cells directly. The total bone volumes were not affected in both the left proximal and distal femora 1 or 4 wk after irradiation in CT analysis (Fig. 2*A*), and the trabecular bone thickness, num-

Author contributions: X.C., X.W., and F.J.F. designed research; D.F., B.Y., L.P., L.X., M.W., W.L., M.A., E.T., and C.Y.W. performed research; J.W. and W.W.L. contributed new reagents/analytic tools; X.C., X.W., and F.J.F. analyzed data; and X.C., X.W., and F.J.F. wrote the paper.

The authors declare no conflict of interest.

*This Direct Submission article had a prearranged editor.

[1]To whom correspondence may be addressed. E-mail: ffrassi@jhmi.edu or xcao11@jhmi.edu.

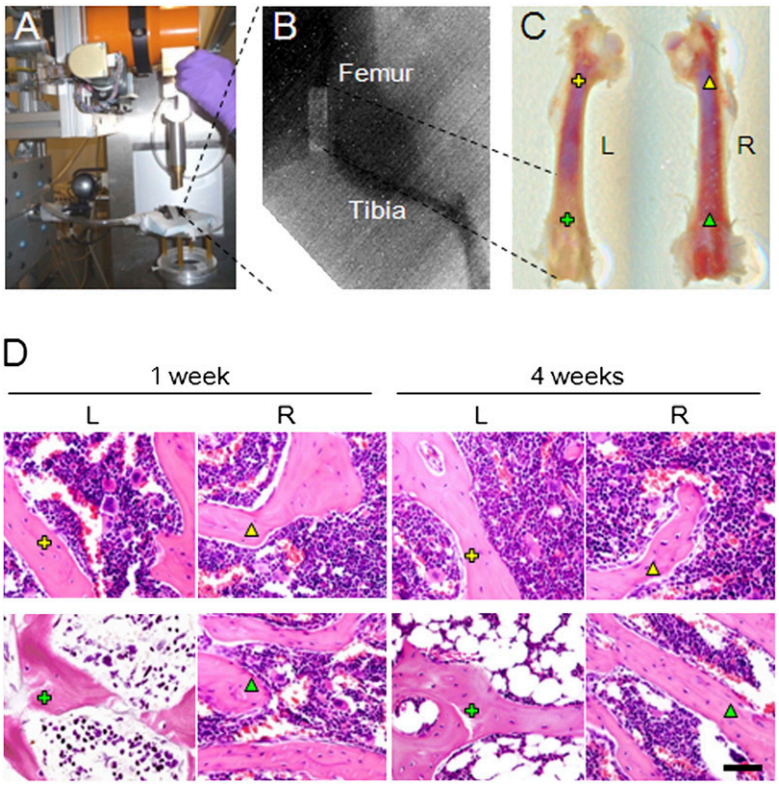

Fig. 1. Local Irradiation on left distal femur. (*A*) SARRP system. (*B*) Radiograph of left lower limb of a mouse that received local irradiation of the distal femur. Light rectangle indicates the beam of X-ray. (*C*) Femora collected from the mice 1 wk after irradiation. (*D*) Light micrographs of H&E staining performed on trabecular bone sections from proximal and distal femora of mice 1 wk and 4 wk after irradiation. Yellow cross indicates left proximal femur, green cross indicates irradiated area of left distal femur, yellow triangle indicates right proximal femur, and green triangle indicates right distal femur. L, left. R, right. (Scale bar: 100 μm.)

ber, and separation were not changed either (Fig. 2 *B–D*). Bone histomorphometry analysis showed that numbers of both osteoclasts and osteoblasts were decreased in the distal femora after irradiation, but no changes were observed in the proximal femora (Fig. 2 *E* and *F*). The results indicate that irradiation affects osteoblasts and osteoclasts in the distal femora, but has no significant effect on differentiated osteoclasts and osteoblasts in the proximal femora (i.e., nonirradiated area).

The effects of irradiation on bone marrow MSCs were examined in CFU-fibroblast (CFU-F) assay with bone marrow cells isolated from left distal femora (i.e., irradiated area) or left proximal femora (i.e., nonirradiated area). No colonies of MSCs were observed in the left proximal femur or distal femur at 1 wk after irradiation, whereas colonies of CFU-F and CFU-osteoblast (CFU-Ob) were observed in the nonirradiated right femur (Fig. 3 *A* and *B*). Interestingly, recovery of MSCs was observed in the left proximal femur at 4 wk, but not for irradiated distal femur. Similar results were observed and osteoblast differentiation potential of MSCs in CFU-Ob assay (Fig. 3 *A* and *C*). The colonies of MSCs in the left and right nonirradiated tibia were not changed (Fig. 3*D*). MSCs have been shown to be mobilized in the circulation in response to tissue damage. We therefore examined the effects of radiation on the levels of MSCs in the circulation. Previously, we have demonstrated the $CD29^+Sca\text{-}1^+CD45^-CD11b^-$ bone marrow stroma are subset of MSCs (19). Flow cytometry analysis of $CD29^+Sca\text{-}1^+CD45^-CD11b^-$MSCs in peripheral blood collected from the mice at 1 and 4 wk after treatment in the irradiation and sham groups indicates that $CD29^+Sca\text{-}1^+CD45^-CD11b^-$MSCs were doubled at 1 wk after irradiation and increased fourfold in 4 wk (Fig. 3*E*). The level of $CD29^+Sca\text{-}1^+CD45^-CD11b^-$MSCs was also increased in proximal femur at 4 wk after irradiation whereas the levels in the right femur and left distal femur were unchanged. The results reveal that bone marrow MSCs can be affected indirectly following irradiation at another site in the bone marrow cavity. The increased level of Sca-1–positive MSCs in response to irradiation suggests that there is a systemic response resulting in mobilization of MSCs for the repair of bone injury.

To examine the mechanism of irradiation-induced damage of bone marrow MSCs, we measured the levels of free radicals in the bone marrow isolated from the irradiated left distal femur, nonirradiated proximal left proximal femur, and right femur by using thiobarbituric acid reactive substances (TBARS) assay. This assay measures the consequences of lipid peroxidation and malondialdehyde specifically. The levels of TBARS were increased threefold at 1 wk and remained at the same level for 4 wk in left distal femora (Fig. 4*A*), whereas the levels were increased at 1 wk and decreased to the basal level at 4 wk in nonirradiated proximal femur (Fig. 4*A*). No changes of TBARS were observed in the right femora (Fig. 4*A*) and circulation (Fig. 4*B*), indicating that the free radicals diffuse to ipsilaterally distal femur through bone medullary channel, leading to MSCs damage. The results also suggest that irradiation produces free radicals that adversely affect the MSCs in both distal and proximal femora, but have no significant effects on differentiated osteoclasts and osteoblasts in the ipsilateral proximal femur (i.e., nonirradiated area).

Vasculatures are essential for the maintenance of MSCs as their niche (20, 21). Bone formation is coupled with angiogenesis (22–24). Angiographic images of microphil-perfused femora were performed to analyze the effects of irradiation on bone marrow vasculatures. The results showed that the blood vessels

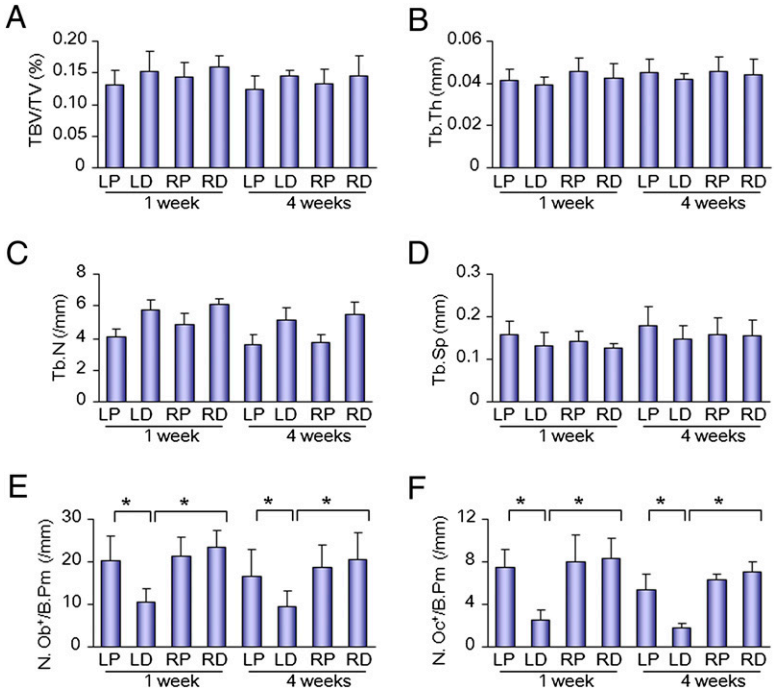

Fig. 2. Bone histomorphometric analysis of trabecular bone from the mice 1 wk and 4 wk after irradiation. Bone volume fraction (BV/TV) (*A*), trabecular thickness (Tb.Th) (*B*), trabecular number (Tb.N) (*C*), trabecular separation (Tb. Sp) (*D*), number of osteoblasts per bone perimeter (N.Ob$^+$/B.Pm) (*E*), and number of osteoclasts per bone perimeter (N.Oc$^+$/B.Pm) (*F*) were measured (LP, left proximal femur; LD, left distal femur; RP, right proximal femur; RD, right distal femur). Data represent the mean ± SEM; $n = 10$ (*$P < 0.05$).

in the irradiated left distal femora were damaged at 1 wk and 4 wk after irradiation, but the vessels were intact in the nonirradiated left proximal femora (Fig. 4*C*). Morphometric analysis showed that vessel volume, thickness, and number were decreased in the distal femur relative to controls (Fig. 4 *D–F*). The results suggest that direct irradiation, not free radical generation, damages the bone marrow vasculatures.

Discussion

In this study, precise irradiation of the mouse distal femur was performed with a unique SARRP built with integration of CT, X-ray, and irradiation in a single treatment platform. The mouse distal half of the femur was precisely irradiated at accuracy of 1 mm. Here, the direct and indirect effects of irradiation on bone injury and bone marrow MSCs were examined in the same mouse femur with common bone marrow cavity. Our results reveal that irradiation can affect bone marrow MSCs indirectly in the proximal femur without direct irradiation. Interestingly, no colony formation of MSCs was observed in CFU-F and CFU-Ob assays in irradiated and nonirradiated areas of the bone marrow, and the levels of free radicals were dramatically increased. Most likely, the free radicals produced during radiation affects the survival, self-renewal, or differentiation of MSCs. Interestingly, the recovery of MSCs colony formation was seen in 4 wk after irradiation in the nonirradiated proximal femur, but not in the irradiated distal femur. Importantly, the vasculatures—the potential niche for stem cells—were destroyed in irradiated areas. Damage of bone marrow vasculatures—the niches for stem cells—likely affects the recovery of MSCs in the irradiated areas, which may explain the refractory nature of bone injury and fractures in patients receiving ionizing radiation to bone. Therefore, our findings suggest that irradiation induces bone injury by producing free radicals that adversely affect microenvironment for MSCs and damaging bone marrow blood vessels.

Bone injury and fractures often occur in patients receiving curative doses of ionizing radiation. These fractures often heal very slowly and sometimes fail to unite. These clinical observations are in accord with our findings in this mouse model and suggest that irradiation damages the bone marrow microenvironment or the niches for stem cells. Recovery of bone injury from ionizing irradiation may occur from repopulation of inhabitant stem cells (14) or repopulation from the systemic circulation. Our results showed that MSCs in the direct irradiated area did not recover, whereas the MSCs in the nonirradiated proximal left proximal femur recovered quickly. The free radicals produced changed the microenvironment in the bone marrow and likely brought the MSCs into a quiescent phase in the nonirradiated area of bone marrow. Stem cells of hematopoietic and mesenchymal origin have been shown in the recovery of ionizing irradiation-induced distal epithelial damage (15–17). The bone marrow with damaged microvasculature is not likely able to retain stem cells and lead to refractory of bone injury and fractures. It has been implicated that mobilization of stem cells in the circulation can occur in response to irradiation (25–27). Indeed, the levels of Sca-1–positive MSCs were increased in the circulation after irradiation. Different markers have been used for MSCs. A recent study revealed that bone barrow MSCs are nestin-positive cells (28). It will be interesting to investigate whether the mobilized Sca-1–positive MSCs are also nestin-positive and if that contributes to the recovery of MSCs in the bone marrow of proximal femur. It will also be interesting to investigate whether the mobilized Sca-1–positive MSCs contribute to the recovery of MSCs in the bone marrow of proximal femur.

The therapeutic potential of bone marrow-derived MSCs has recently been implicated. Not only are these cells able to migrate to injured tissues, but they also are able to differentiate into different phenotypes according to the tissues in which they reside (29). Furthermore, it has been shown that MSCs of bone marrow

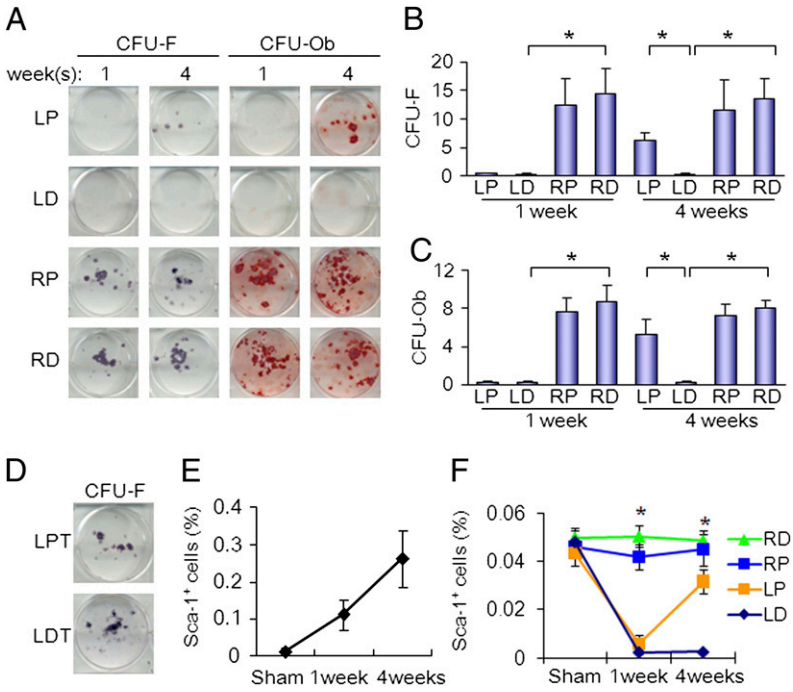

Fig. 3. Effects of local irradiation on potential of MSCs. (*A*) Colonies formed from harvested bone marrow of femora of the mice as indicated in CFU-F and CFU-Ob assays (1×10^5 bone marrow nucleated cells were plated into six-well plates). (*B* and *C*) The colony-forming efficiency was determined by number of colonies per 10^5 marrow cells plated. Data represent the mean ± SEM of triplicate cultures of bone marrow nucleated cells from five individual mice (*$P < 0.05$). (*D*) Colonies formed from harvested bone marrow of left tibia of the mice as indicated in CFU-F assay. (*E* and *F*) FACS analysis of the sorted Sca-1, CD29, CD45, and CD11b cells from the peripheral blood plasma (*E*) and the bone marrow cell suspension (*F*) obtained from the mice. Data represent the mean ± SEM; $n = 5$.

origin could hasten hematopoietic recovery and provide a better tool for cell therapy if applied autologously to patients who undergo irradiation (30, 31). Thus, improving bone marrow microenvironment and accelerating vasculogenesis could be a potential treatment for patients with radiation-induced bone injury.

Methods

Mice. C57BL/6J (WT) mice were purchased from Charles River. Male mice 8 wk of age were anesthetized by inhalation of isoflurane during the procedure and immobilized using fixtures. SARRP developed by researchers at the Department of Radiation Oncology at Johns Hopkins University was used to irradiate the mice. A clinically applicable dose rate (4 Gy min^{-1}) was delivered by using the 225-kVp setting with a 3.0-mm focal spot with a maximum 13 mA beam current. Irradiation was once per day, and the total dose is 20 Gy. All animals were maintained in the animal facility of the Johns Hopkins University School of Medicine. The experimental protocol was reviewed and approved by the institutional animal care and use committee of the Johns Hopkins University.

Histochemistry and Histomorphometric Analysis. At the time of euthanasia, the bone tissues were resected and fixed in 10% buffered formalin for 48 h, decalcified in 10% EDTA (pH 7.0) for 20 d, and embedded in paraffin. Longitudinally oriented sections of bone 4 μm thick, including the metaphysis and diaphysis, were processed for H&E staining. Sections were microphotographed to perform histomorphometric measurements on the highlighted areas of the bone displayed on the digitalized image. Quantitative histomorphometric analysis was conducted in a blinded fashion with OsteoMeasureXP Software (OsteoMetrics). Two-dimensional parameters of trabecular bone were measured in a 2-mm square 1 mm distal to the lowest point of the growth plate in the trabecular bone.

CFU-F and CFU-Ob Assays. At the time of euthanasia, the femora were cut in half into proximal and distal pieces and bone marrow from medullary cavities were collected individually, and cell number was determined after removal of red blood cells with Zapoglobin (Coulter). The number of CFU-Fs and CFU-Obs in murine bone marrow isolates and in cultures of bone marrow cells was determined in cocultures with irradiated guinea pig marrow cells as reported. Briefly, marrow cells were obtained from the femurs and tibiae of 2-mo-old female Hartley guinea pigs by flushing with a 22-gauge needle and resuspended. Cells were γ-irradiated with a ^{57}Co source for 50 min at 1.2 Gy/min as reported. After rinsing by centrifugation, cells were resuspended in minimum essential medium-α with 20% FBS, counted, and cultured at 2.5×10^6 per well of a six-well plate.

For assay of CFU-F and CFU-Ob number, 1×10^5 murine marrow cells were plated into six-well plates in 3 mL minimum essential medium-α supplemented with glutamine (2 mM), penicillin (100 U/mL), streptomycin sulfate (100 μg/mL), and 20% lot-selected FBS. Duplicate cultures were established. After 2 to 3 h of adhesion, unattached cells were removed, and 2.5×10^6 irradiated guinea pig feeder cells (provided by Brendan J. Canning, Johns Hopkins Asthma and Allergy Center, Baltimore) were added to cultivation medium of adherent cultures just after washing. On day 14, cultures were fixed and stained with 0.5% crystal violet. The colonies containing 50 or more cells were counted. For CFU-Ob assay, the cells were cultured with osteogenic medium as described earlier for 21 d and analyzed with Alizarin red staining. The colony-forming efficiency was determined by number of colonies per 10^5 marrow cells plated.

FACS Analysis. Cells aliquots were incubated for 20 min at 4 °C with antibodies conjugated by phycoerythrin, FITC, peridinin chlorophyll protein, and allophycocyanin against mouse Sca-1, CD29, CD45, and CD11b (Biolegend). Acquisition was performed on a FACSAria sorter (BD Biosciences), and analysis was performed using a FACS DIVE software, version 6.1.3 (BD Biosciences).

Measurement of Lipid Oxidation. Peripheral venous blood was drawn into syringes containing preservative-free heparin (25 U/mL; Gibco/Life Technologies) and centrifuged at $1,200 \times g$ for 10 min at 5 °C to 10 °C to isolate the plasma. Bone marrow samples were collected into preservative-free heparinized saline solution (25 U/mL) and centrifuged at 3,500 rpm for 10 min at 5 °C to 10 °C to isolate bone marrow plasma. Plasma lipid oxidation was assessed by determining the level of TBARS by using a TBARS assay kit (Zeptometrix).

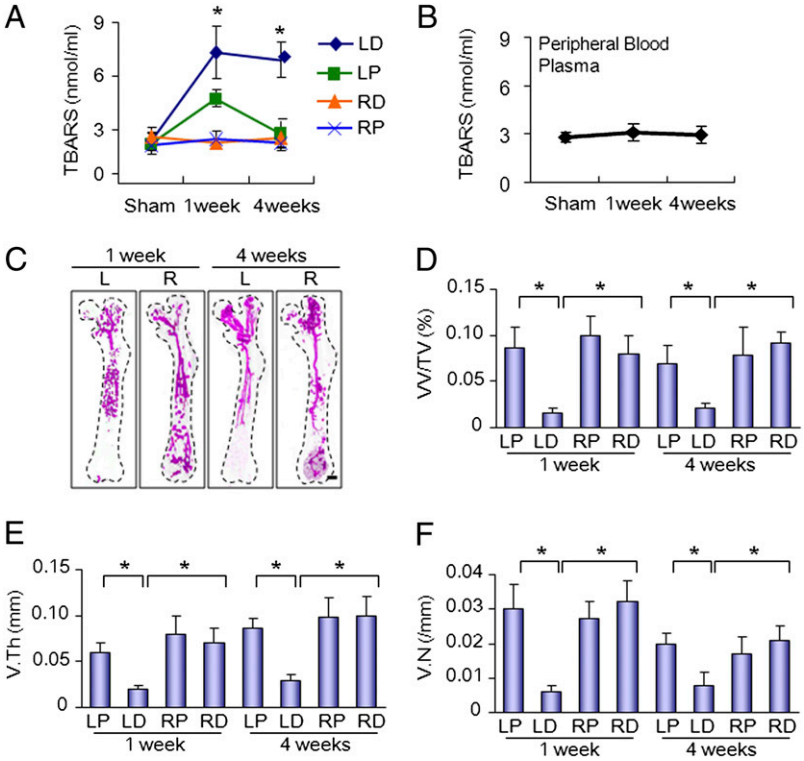

Fig. 4. Effects of local irradiation on the production of free radicals and angiogenesis. Free radicals were assessed in both bone marrow (*A*) and peripheral blood (*B*) before irradiation and 1 wk and 4 wk after irradiation detected by TBARS assay. (*C*) Representative 3D micro-CT images of femora from the mice after local irradiation. (Scale bar: 1 mm.). (*D–F*) Quantitative micro-CT angiography analysis. Vascular volume fraction (VV/TV) (*D*), vascular thickness (V.Th) (*E*), and vascular number (V.N) (*F*) were measured. Data represent the mean ± SEM; $n = 10$ (*$P < 0.05$).

Micro-CT Angiography Analysis. Blood vessels in bone were imaged by angiography of microphil-perfused long bones. The thoracic cavity was opened, and the inferior vena cava was severed after animals were killed. The vasculature was flushed with 0.9% normal saline solution containing heparin sodium (100 U/mL) through a needle inserted into the left ventricle. The specimens were pressure fixed with 10% neutral buffered formalin. Formalin was flushed from the vessels by using heparinized saline solution, and the vasculature was injected with a radiopaque silicone rubber compound containing lead chromate (Microfil MV-122; Flow Tech). Samples were stored at 4 °C overnight for contrast agent polymerization. Mouse femurs were dissected from the specimens and soaked for 4 d in 10% neutral buffered formalin to ensure complete tissue fixation. Specimens were subsequently treated for 48 h in a formic acid-based solution (Cal-Ex II) to decalcify the bone and facilitate image thresholding of the femoral vasculature from the surrounding tissues. Images were obtained using a high resolution (9-μm isotropic voxel size) micro-CT imaging system (MicroCT40; Scanco). A threshold of 306 was initially chosen based on visual interpretation of thresholded 2D tomograms.

Statistics. Data are presented as mean ± SEM and were analyzed using a one-way ANOVA followed by Dunnett test.

1. Costantino PD, Friedman CD, Steinberg MJ (1995) Irradiated bone and its management. *Otolaryngol Clin North Am* 28:1021–1038.
2. Jegoux F, Malard O, Goyenvalle E, Aguado E, Daculsi G (2010) Radiation effects on bone healing and reconstruction: interpretation of the literature. *Oral Surg Oral Med Oral Pathol Oral Radiol Endod* 109:173–184.
3. Baxter NN, Habermann EB, Tepper JE, Durham SB, Virnig BA (2005) Risk of pelvic fractures in older women following pelvic irradiation. *JAMA* 294:2587–2593.
4. Gerson SL (1999) Mesenchymal stem cells: No longer second class marrow citizens. *Nat Med* 5:262–264.
5. Prockop DJ (1997) Marrow stromal cells as stem cells for nonhematopoietic tissues. *Science* 276:71–74.
6. Jiang Y, et al. (2002) Pluripotency of mesenchymal stem cells derived from adult marrow. *Nature* 418:41–49.
7. Kawada H, et al. (2004) Nonhematopoietic mesenchymal stem cells can be mobilized and differentiate into cardiomyocytes after myocardial infarction. *Blood* 104: 3581–3587.
8. Lee KD, et al. (2004) In vitro hepatic differentiation of human mesenchymal stem cells. *Hepatology* 40:1275–1284.
9. Garrett RW, Emerson SG (2009) Bone and blood vessels: The hard and the soft of hematopoietic stem cell niches. *Cell Stem Cell* 4:503–506.
10. Yin T, Li L (2006) The stem cell niches in bone. *J Clin Invest* 116:1195–1201.
11. Mauch P, et al. (1995) Hematopoietic stem cell compartment: Acute and late effects of radiation therapy and chemotherapy. *Int J Radiat Oncol Biol Phys* 31: 1319–1339.
12. Dickhut A, et al. (2005) Mesenchymal stem cells obtained after bone marrow transplantation or peripheral blood stem cell transplantation originate from host tissue. *Ann Hematol* 84:722–727.
13. Rieger K, et al. (2005) Mesenchymal stem cells remain of host origin even a long time after allogeneic peripheral blood stem cell or bone marrow transplantation. *Exp Hematol* 33:605–611.
14. Greenberger JS, Epperly M (2009) Bone marrow-derived stem cells and radiation response. *Semin Radiat Oncol* 19:133–139.
15. Epperly MW, et al. (2004) Bone marrow origin of cells with capacity for homing and differentiation to esophageal squamous epithelium. *Radiat Res* 162:233–240.
16. Greenberger JS, Epperly MW (2007) Review. Antioxidant gene therapeutic approaches to normal tissue radioprotection and tumor radiosensitization. *In Vivo* 21: 141–146.
17. Krause DS, et al. (2001) Multi-organ, multi-lineage engraftment by a single bone marrow-derived stem cell. *Cell* 105:369–377.
18. Deng H, et al. (2007) The small-animal radiation research platform (SARRP): Dosimetry of a focused lens system. *Phys Med Biol* 52:2729–2740.
19. Tang Y, et al. (2009) TGF-beta1-induced migration of bone mesenchymal stem cells couples bone resorption with formation. *Nat Med* 15:757–765.
20. Crisan M, et al. (2008) A perivascular origin for mesenchymal stem cells in multiple human organs. *Cell Stem Cell* 3:301–313.
21. Shi S, Gronthos S (2003) Perivascular niche of postnatal mesenchymal stem cells in human bone marrow and dental pulp. *J Bone Miner Res* 18:696–704.
22. Schipani E, Maes C, Carmeliet G, Semenza GL (2009) Regulation of osteogenesis-angiogenesis coupling by HIFs and VEGF. *J Bone Miner Res* 24:1347–1353.
23. Street J, et al. (2002) Vascular endothelial growth factor stimulates bone repair by promoting angiogenesis and bone turnover. *Proc Natl Acad Sci USA* 99:9656–9661.
24. Wang Y, et al. (2007) The hypoxia-inducible factor alpha pathway couples angiogenesis to osteogenesis during skeletal development. *J Clin Invest* 117:1616–1626.

25. Harrison DE, Astle CM, Delaittre JA (1978) Loss of proliferative capacity in immunohemopoietic stem cells caused by serial transplantation rather than aging. *J Exp Med* 147:1526–1531.
26. Harrison DE, Astle CM (1982) Loss of stem cell repopulating ability upon transplantation. Effects of donor age, cell number, and transplantation procedure. *J Exp Med* 156:1767–1779.
27. Werts ED, Gibson DP, Knapp SA, DeGowin RL (1980) Stromal cell migration precedes hemopoietic repopulation of the bone marrow after irradiation. *Radiat Res* 81:20–30.
28. Méndez-Ferrer S, et al. (2010) Mesenchymal and haematopoietic stem cells form a unique bone marrow niche. *Nature* 466:829–834.
29. Horwitz EM, et al. (2002) Isolated allogeneic bone marrow-derived mesenchymal cells engraft and stimulate growth in children with osteogenesis imperfecta: Implications for cell therapy of bone. *Proc Natl Acad Sci USA* 99:8932–8937.
30. Koç ON, et al. (1999) Bone marrow-derived mesenchymal stem cells remain host-derived despite successful hematopoietic engraftment after allogeneic transplantation in patients with lysosomal and peroxisomal storage diseases. *Exp Hematol* 27:1675–1681.
31. Koç ON, et al. (2000) Rapid hematopoietic recovery after coinfusion of autologous-blood stem cells and culture-expanded marrow mesenchymal stem cells in advanced breast cancer patients receiving high-dose chemotherapy. *J Clin Oncol* 18:307–316.